

The first electron beam polarization measurement with a diamond micro-strip detector

A. Narayan¹, D. Dutta¹, V. Tvaskis^{2,3}, D. Gaskell⁴, J. W. Martin², A. Asaturyan⁵, J. Benesch⁴, G. Cates⁶, B. S. Cavness⁷, J. C. Cornejo⁸, M. Dalton⁶, W. Deconinck⁸, L. A. Dillon-Townes⁴, G. Hays⁴, E. Ihloff⁹, D. Jones⁶, R. Jones¹⁰, S. Kowalski¹¹, L. Kurchaninov¹², L. Lee¹², A. McCreary¹³, M. McDonald², A. Micherdzinska², A. Mkrtchyan⁵, H. Mkrtchyan⁵, V. Nelyubin⁶, S. Page³, K. Paschke⁶, W. D. Ramsay¹², P. Solvignon⁴, D. Storey², A. Tobias⁶, E. Urban¹⁴, C. Vidal⁹, P. Wang³, and S. Zhamkotchyan⁵

¹Mississippi State University, Mississippi State, MS 39762, USA

²University of Winnipeg, Winnipeg, MB R3B 2E9, Canada

³University of Manitoba, Winnipeg, MB R3T 2N2, Canada

⁴Thomas Jefferson National Accelerator Facility, Newport News, VA 23606, USA

⁵Yerevan Physics Institute, Yerevan, 375036, Armenia

⁶University of Virginia, Charlottesville, VA 22904, USA

⁷Angelo State University, San Angelo, TX 76903, USA

⁸College of William and Mary, Williamsburg, VA 23186, USA

⁹MIT Bates Linear Accelerator Center, Middleton, MA 01949, USA

¹⁰University of Connecticut, Storrs, CT 06269, USA

¹¹Massachusetts Institute of Technology, Cambridge, MA 02139, USA

¹²TRIUMF, Vancouver, BC V6T 2A3, Canada

¹³University of Pittsburgh, Pittsburgh, PA 15260, USA and

¹⁴Hendrix College, Conway, AR 72032, USA

A diamond multi-strip detector was used for the first time, to track Compton scattered electrons in a new electron beam polarimeter in the experimental Hall C at Jefferson Lab. We report the first high precision beam polarization measurement with electrons detected in diamond multi-strip detectors. The analysis technique leveraged the high resolution of the detectors and their proximity to the electron beam ($\gtrsim 0.5$ cm). The polarization was measured with a statistical precision of $< 1\%$ /hr, and a systematic uncertainty of 0.59%, for a 1.16 GeV electron beam with currents up to 180 μ A. This constitutes the highest precision achieved for polarization measurement of few-GeV electron beams.

PACS numbers:

INTRODUCTION

High precision nuclear physics experiments using polarized electron beams rely on accurate knowledge of beam polarization to achieve their ever improving precision. A parity violating electron scattering (PVES) experiment in the experimental Hall C at Jefferson Lab (JLab), known as the Q_{weak} experiment, is the most recent example [1, 2]. The goal of the Q_{weak} experiment is to measure the Standard Model parameter known as the weak mixing angle, at a low energy (relative to the Z^0 mass) with unprecedented precision. With a goal of $< 1\%$ uncertainty, determination of electron beam polarization is one of the largest experimental uncertainties of the Q_{weak} experiment. The experiment utilized an existing Møller polarimeter [2, 3] and a new Compton polarimeter to monitor the electron beam polarization. The Compton polarimeter is the only polarimeter at JLab Hall C that can non-destructively monitor the beam polarization at the exact running conditions of the Q_{weak} experiment.

The use of Compton scattered electrons and/or back-scattered photons to measure the Compton asymmetry and thereby the electron beam polarization, is a well established polarimetry technique [4–9]. Most previ-

ous Compton polarimeters, other than the one used in the SLD experiment [6], relied primarily on detection of the scattered photons to measure the beam polarization. The SLD Compton polarimeter, which detected scattered electrons (and used detection of photons as a cross-check), was operated at a beam energy of 50 GeV and reported a precision of 0.5%. The relatively low energy of the electron beam at JLab leads to a smaller Compton analyzing power, and makes it significantly more challenging to achieve the same level of precision. Nonetheless, the Compton polarimeter in Hall A at Jefferson Lab has reported a relative precision of $\sim 1\%$ by detecting the Compton scattered electrons at a beam energy of 3 GeV [10].

The JLab Hall C Compton polarimeter detects the scattered electrons in a set of tracking detectors. The low energy of the electron beam (1.16 GeV) and other operating parameters of the Q_{weak} experiment, presented the most challenging set of conditions to achieve the goal of $< 1\%$ uncertainty in measurement of the beam polarization. For example, it constrains the tracking detector to be placed as close as 0.5 cm from the electron beam. Further, the polarimeter was operated at the highest beam current (180 μ A) ever used by any experiment at JLab

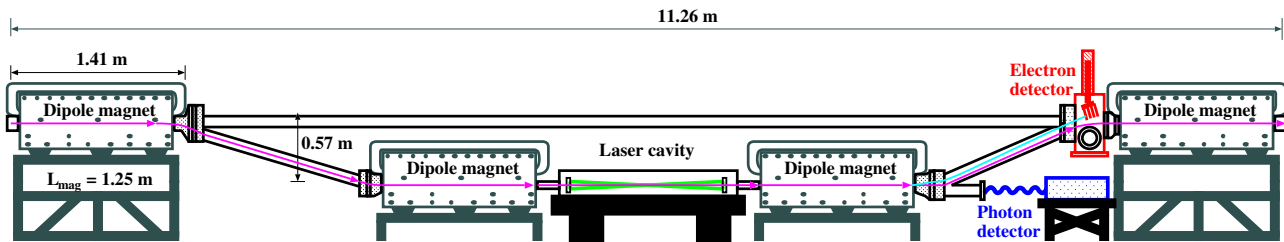


FIG. 1: Schematic of the JLab Hall C Compton polarimeter.

48 and ran for over 5000 hrs, thereby subjecting the elec- 90
 49 tron detectors to a rather large cumulative radiation dose 91
 50 (> 10 MRad, just from electrons). In order to withstand 92
 51 the large radiation dose, a novel set of diamond micro- 93
 52 strip detectors were used to track the scattered electrons. 94

53 The use of *natural* diamond in the detection of charged 95
 54 particles and radiation has a long history, however, the 96
 55 use of synthetic diamond grown through a process known 97
 56 as “chemical vapor deposition” (CVD), is a relatively 98
 57 recent development. Detailed reviews of diamond as 99
 58 charged particle detectors can be found in [11–13]. Thin- 100
 59 sheets of centimeter-sized diamond are grown using the 101
 60 CVD process and the plates of diamond are then turned 102
 61 into charged particle detectors by depositing suitable 103
 62 electrodes on them [14]. A minimum ionizing particle 104
 63 (MIP) passing through a thin layer of diamond leaves be- 105
 64 hind a trail of electron-hole pairs. In the presence of an 106
 65 external electric field the electrons and holes move away 107
 66 from one another, and this movement of the charges in- 108
 67 duces a signal in the external circuit attached to the elec- 109
 68 trodes. The signal per electron-hole pair is proportional 110
 69 to the mean separation of the electron and hole before 111
 70 they become trapped in the material. 112

71 Compared to the more commonly used silicon detec- 113
 72 tor, the signal size in a diamond detector is significantly 114
 73 smaller, but the higher electron and hole mobility of 115
 74 diamond leads to a faster and shorter duration signal. 116
 75 However, the well-established radiation hardness of dia-
 76 mond [15, 16] is by far the most important consideration
 77 for the use of diamond detectors in nuclear and particle
 78 physics experiments. In this letter we report the first use
 79 of diamond micro-strip detectors as a tracking detector
 80 in a nuclear physics experiment and the first high pre-
 81 cision measurement of electron beam polarization with
 82 this device.

83 THE HALL C COMPTON POLARIMETER

84 A schematic of the Compton polarimeter in Hall C
 85 at JLab is shown in Fig. 1, it consists of four identical
 86 dipole magnets forming a magnetic chicane that displaces
 87 a 1.16 GeV electron beam vertically downward by 57 cm.
 88 A high intensity ($\sim 1 - 2$ kW) beam of $\sim 100\%$ circularly 117
 89 polarized photons is provided by an external low-gain 118

Fabry-Pérot laser cavity which consists of an 85 cm long
 optical cavity with a gain between 100 and 200, coupled
 to a green (532 nm), continuous wave, 10 W laser (Co-
 herent VERDI). The laser light is focused at the inter-
 action region ($\sigma_{\text{waist}} \sim 180 \mu\text{m}$), and it is larger than
 the electron beam envelope ($\sigma_{x/y} \sim 40 \mu\text{m}$ when opti-
 mally tuned). The degree of circular polarization was
 determined by two methods; first by monitoring the po-
 larization state of the transmitted laser light and using
 a transfer function to translate it to the Compton in-
 teraction point, and second a more precise method of
 measuring the leakage of the back-reflected power from
 the laser cavity.

The laser was operated in ~ 90 second cycles, where
 it is active for ~ 60 s (laser on period) and blocked off
 (laser off period) for the rest of the cycle. The laser off
 data was used to measure the background. The helicity
 of the laser beam was reversed very infrequently (6 times
 during the entire experiment).

The maximum scattered photon energy was approxi-
 mately 46 MeV. A calorimeter consisting of a 2×2 ma-
 trix of $3 \text{ cm} \times 3 \text{ cm}$ PbWO_4 scintillating crystals at-
 tached to a single photo-multiplier tube was used to measure the
 scattered photon energy. The signal from the photon de-
 tector was digitally integrated with no thresholds over a
 full helicity state (~ 1 ms) using a 200 MHz flash analog
 to digital converter.

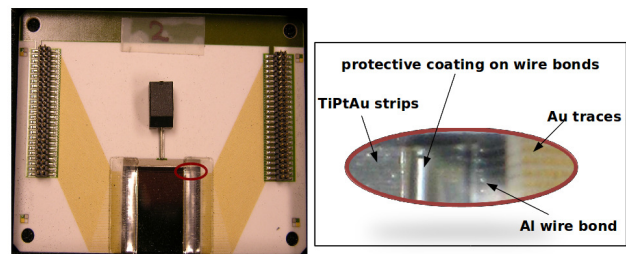


FIG. 2: A CVD diamond plate mounted on an alumina sub-
 strate which forms a single detector plane (left). The red oval
 indicates the area that has been shown in the enlarged view
 (right).

The Compton scattered electrons were momentum an-
 alyzed by the third dipole magnet of the chicane. The

119 maximum separation between the primary electron beam₁₅₈
 120 and the Compton scattered electrons, just in front of₁₅₉
 121 the fourth dipole, was ~ 17 mm. The deflection of the₁₆₀
 122 scattered electron with respect to the primary electron₁₆₁
 123 beam, from the maximum down to distances as small as₁₆₂
 124 ~ 5 mm, was tracked by a set of four diamond micro-strip₁₆₃
 125 detectors. This range allowed the detection of a large
 126 fraction of the Compton electron spectrum, from beyond
 127 the kinematic maximum (strip 55 in Fig. 3) down past the
 128 zero-crossing point of the Compton asymmetry. The elec-₁₆₄
 129 tron detectors are made from 21 mm \times 21 mm \times 0.5 mm
 130 plates of CVD diamond [17]. Each diamond plate has₁₆₅
 131 96 horizontal metalized electrode strips with a pitch of₁₆₆
 132 200 μm (180 μm of metal and 20 μm of gap) on one side₁₆₇
 133 (front) and a single metalized electrode covering the en-₁₆₈
 134 tire diamond surface on the opposite (back) side. Details₁₆₉
 135 about these detectors can be found in Ref. [2]. A single₁₇₀
 136 detector plane is shown in Fig 2. 171

137 Only 3 out of the 4 detector planes were operational₁₇₂
 138 during the experiment. A typical charge normalized₁₇₃
 139 Compton electron spectrum, as well as a charge normal-₁₇₄
 140 ized background spectrum, is shown in Fig 3. A statis-₁₇₅
 141 tical precision of $< 1\%$ per hour was routinely achieved₁₇₆
 142 with these detectors. By comparing the expected to the₁₇₇
 143 observed rates, the detector efficiency was estimated to₁₇₈
 144 be $\sim 70\%$. The large inefficiency is mostly due to the
 145 large separation between the detector and the readout
 146 electronics. Over the 2 year period of the Q_{weak} experi-
 147 ment, the detectors were exposed to a radiation dose of \sim
 148 10 MRad (without including the dose from Synchrotron
 149 radiation). No significant degradation of the signal size
 150 was observed during this period, demonstrating the ra-
 151 diation hardness of the diamond detectors.

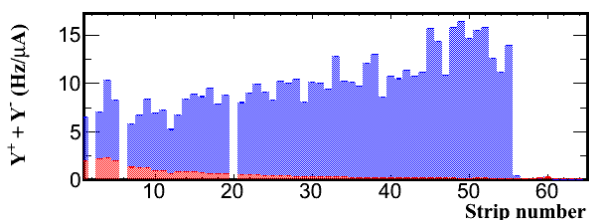


FIG. 3: A typical spectrum of normalized yield ($Y^+ + Y^-$) from the detector strips for a single detector plane. The charge normalized background subtracted spectrum is shown in blue and the charge normalized background is shown in red.

152 DATA REDUCTION AND RESULTS

153 The electron beam helicity was reversed at a rate of
 154 960 Hz in a pseudo-random sequence. In addition a₁₇₉
 155 half-wave plate in the polarized electron photo emission₁₈₀
 156 source [18] was inserted or removed about every 8 hours₁₈₁
 157 to reverse the beam helicity relative to the polarization

of the source laser. The background yield measured during the laser-off period was subtracted from the laser-on yield for each electron helicity state, and a charge normalized Compton yield for each detector strip was obtained for the two electron helicities (as shown in Fig. 3). The measured asymmetry was built from these yields using,

$$A_{exp} = \frac{Y^+ - Y^-}{Y^+ + Y^-}, \quad (1)$$

where $Y^\pm = \frac{N_{on}^\pm}{Q_{on}^\pm} - \frac{N_{off}^\pm}{Q_{off}^\pm}$ is the charge normalized Compton yield for each detector strip, $N_{on/off}^\pm$ and $Q_{on/off}^\pm$ are the detector counts and the beam charge accumulated during the laser on/off period for the two electron helicity states (\pm), respectively. The Compton yields were averaged over two different time intervals, 1 million helicity cycles and 1 laser cycle. The asymmetry extracted from both time intervals was found to be consistent with each other. A typical asymmetry spectrum during the laser-on and -off period for one detector plane is shown in Fig. 4. The background asymmetry is consistent with zero within the statistical uncertainties, and given the large signal-to-background ratio (see Fig. 3) the dilution to the measured asymmetry due to the background is negligible.

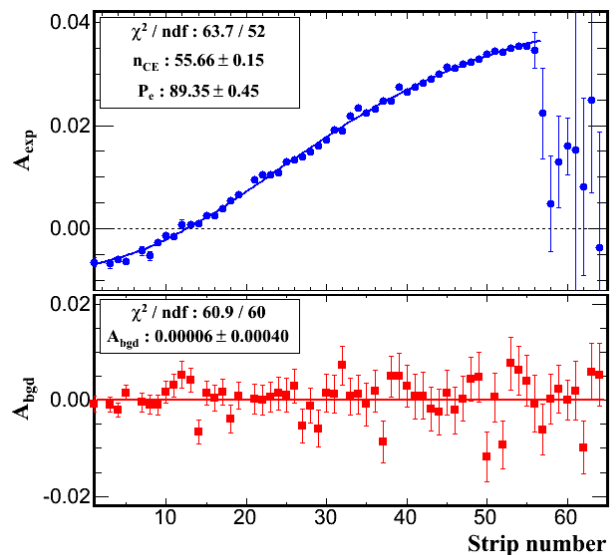


FIG. 4: The measured asymmetry as function of detector strip number for a single detector plane during the laser-on period (top) and the background asymmetry from the laser-off period (bottom). The dashed line in the top panel corresponds to $A_{exp} = 0$. The solid blue line (top) is a fit to Eq. 2 and the solid red line (bottom) is a fit to a constant value. Only statistical uncertainties are shown in this figure.

The electron beam polarization P_e was extracted by fitting the measured asymmetry to a calculated Compton asymmetry using;

$$A_{exp}(y_n) = P_e P_\gamma A_{th}(y_n), \quad (2)$$

182 where P_γ is the polarization of the photon beam, A_{th} is210
 183 the calculated Compton asymmetry and y_n is the scat-211
 184 tered electron displacement along the detector plane for212
 185 the n -th strip. The Compton asymmetry, (A_{th}), is typi-213
 186 cally calculated as a function of the dimensionless quan-214
 187 tity $\rho = E_\gamma/E_\gamma^{max}$, where E_γ and E_γ^{max} is the energy215
 188 of the back-scattered photon and its maximum value, re-216
 189 spectively. However, in order to directly compare with217
 190 the measured asymmetry, ρ was mapped to the displace-218
 191 ment of the scattered electron along the detector plane,219
 192 (y_n). The scattered electron displacement y_n in mm is220
 193 given by, $y_n = y_{max} - 0.2 * (n_{CE} - n)$, where y_{max} is the221
 194 maximum displacement of the scattered electrons from222
 195 the primary beam (the Compton Edge), the width of each223
 196 strip is 0.2 mm, and n_{CE} is the strip number correspond-224
 197 ing to the maximum displaced electrons. The maximum225
 198 displacement, (y_{max}), was determined from the dimen-226
 199 sions and the dispersion of the chicane magnets, and the227
 200 exact location of the detectors with respect to the third228
 201 dipole.

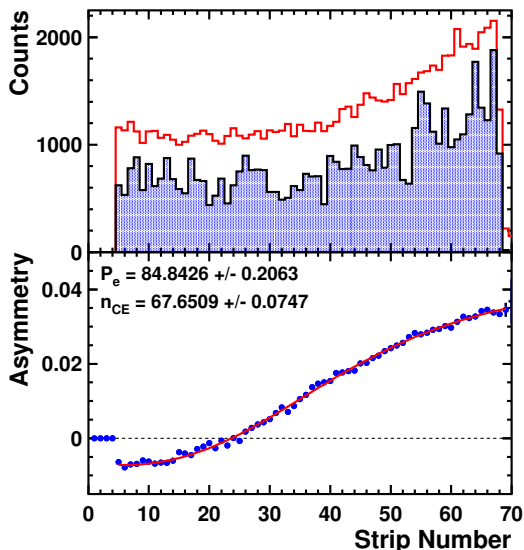


FIG. 5: (top) A typical Monte Carlo simulated Compton spectrum for a single detector plane, with (blue, shaded) and without (red) detector inefficiency. The counts have been scaled by a factor of 10^{-3} . (bottom) The Compton asymmetry extracted from the simulated spectrum including detector inefficiency (blue circles), and a two parameter fit to the calculated asymmetry (red line). The input asymmetry was 85%.

202 The measured asymmetry (A_{exp}) for each ~ 1 hour
 203 long interval (run) was fit to Eq. 2 for each detector strip,
 204 with the beam polarization (P_e) and the non-integer strip
 205 number corresponding to the maximum displaced elec-
 206 trons (n_{CE}) as the two independent parameters of the fit.244
 207 The number of degrees of freedom was typically between245
 208 50 – 60, which was made possible by the high resolution246
 209 of the detector, and the proximity of the detector to the247

primary electron beam. The detection of a large fraction
 of the Compton electron spectrum, spanning both sides
 of the zero crossing of the Compton asymmetry, significantly
 improving the robustness of the fit and the analysis
 technique. A typical fit is shown in Fig. 4. The χ^2 per
 degree-of-freedom of the fit ranges between 0.8 – 1.5 for
 all production runs reported here.

A full Monte Carlo simulation of the Compton polarimeter
 was built using the Geant3 [19] detector simulation package.
 In addition to Compton scattering, the simulation included
 backgrounds from beam-gas interactions and beam halo
 interactions in the chicane elements. The simulation also
 incorporated the effects of detector inefficiency, track-
 finding trigger, and electronic noise. A typical simulated
 strip-hit spectrum (with and without detector inefficiency),
 and the asymmetry extracted from simulated spectra are
 shown in Fig. 5. The simulation was used to validate the
 analysis procedure and to study a variety of sources of
 systematic uncertainties. For each source, the relevant
 parameter was varied within the expected range of uncer-
 tainty, and the change in the extracted polarization was
 listed as its contribution to the systematic uncertainty.
 The list of contributions is shown in Table I.

The Monte Carlo simulation demonstrated that secondary
 particles knocked out by the Compton scattered electron
 passing through the first plane produced a 0.4% change
 in polarization in the subsequent planes. Such a plane-
 to-plane variation was indeed observed in the polarization
 extracted from the second and third planes. One can
 calculate a correction for the later planes but at the cost
 of a slightly higher systematic uncertainty and hence only
 the results from the first detector plane are quoted here.

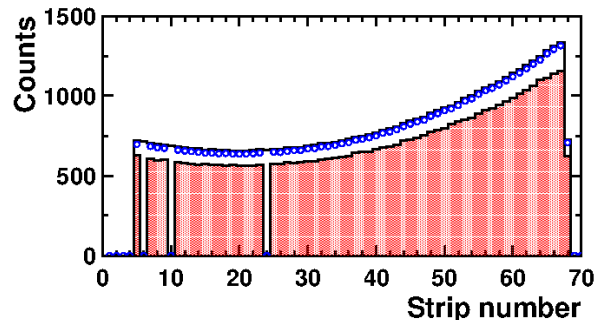
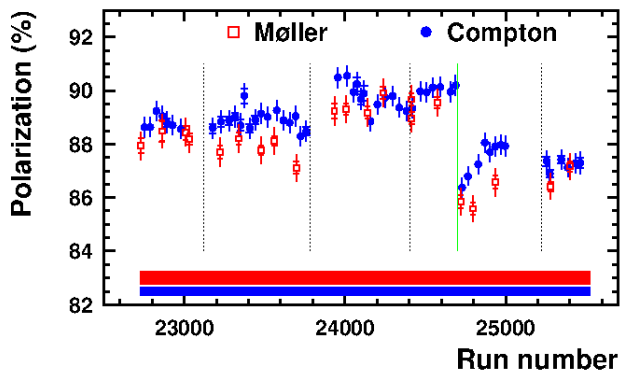


FIG. 6: A typical Modelsim simulated spectrum (without noise and detector inefficiency) of a single detector plane, for un-triggered (blue open circles) and triggered (red shaded) DAQ modes. The input spectrum is shown as the black histogram. The counts have been scaled by a factor of 10^{-3} .

There are several sources of inefficiencies associated with
 the data acquisition (DAQ) system, such as, the algorithm
 used to identify electron tracks and form the trigger,
 and the dead-time due to the hold off (busy) pe-

248 riod in the DAQ. The entire DAQ chain was simulated on 279
 249 a platform called Modelsim [20]. While in Monte Carlo 280
 250 simulations, events are generated based on the probabil- 281
 251 ity distribution for the relevant physics process, in con- 282
 252 trast Modelsim is a simulation technique based on time 283
 253 steps. It employs the same firmware, written in the hard- 284
 254 ware description language for very high speed integrated 285
 255 circuits (VHDL), that operated the field programmable 286
 256 gate array (FPGA) based logic modules [21] in the Com-
 257 pton DAQ. A front end module, called “test-bench”, was
 258 used to control the DAQ firmware in the simulation.

259 The test bench includes signal generators that mimic
 260 the electron, the background and the noise signals, along
 261 with a detailed accounting of delays due to the signal
 262 pathways and the electronic chain external to the FPGA.
 263 Fig. 6 shows the output spectra from a Modelsim simula-
 264 tion, for the triggered and the un-triggered modes, along
 265 with the input spectrum. Noise and detector inefficien-
 266 cies were not included in these simulations as they were
 267 shown to have minimal impact on the determination of
 268 the DAQ inefficiencies. The small difference between the
 269 input and the un-triggered counts is a result of the DAQ
 270 being disabled during helicity reversal. The difference
 271 between the triggered and the un-triggered counts is due
 272 to the DAQ inefficiency. The average DAQ inefficiency
 273 was found to be directly related to the aggregate detector
 274 rate.



287
 288
 289
 290
 291
 292
 293
 294
 295
 296
 297
 298
 299
 300
 301
 302
 FIG. 7: The extracted beam polarization as a function of run-
 number averaged over 30 hour long periods, during the second
 run period of the Q_{weak} experiment (blue, circle). Also shown
 are the results from the intermittent measurements with the
 Møller polarimeter [2, 3] (red, open square). The inner error
 bars show the statistical uncertainty while the outer error bar
 is the quadrature sum of the statistical and point-to-point
 systematic uncertainties. The solid bands show the additional
 normalization/scale type systematic uncertainty. The dashed
 and solid (green) vertical lines indicate changes at the electron
 source.

295 The DAQ simulation was used to determine the cor-
 296 rection to the detector yield for each 1 hr run, based on
 297 the aggregate detector rate during the run. The DAQ
 298 inefficiency correction resulted in $< 1\%$ change in the ex-

tracted polarization. The validity of the corrections and
 the systematic uncertainty due to the corrections (listed
 in Table I) was determined by comparing the polariza-
 tion extracted from triggered vs un-triggered data over a
 wide range of beam currents (rates) and several different
 trigger conditions. Thus, the Modelsim simulation pro-
 vided a robust method to determine the inefficiency of
 the DAQ.

TABLE I: Systematic Uncertainties

Source	Uncertainty	det.P/P%
Laser Polarization	0.18	0.18
Plane to Plane	secondaries	0.00
magnetic field	0.0011 T	0.13
beam energy	1 MeV	0.08
detector z position	1 mm	0.03
inter plane trigger	1-3 plane	0.19
trigger clustering	1-8 strips	0.01
detector tilt(w.r.t x)	1 degree	0.03
detector tilt(w.r.t y)	1 degree	0.02
detector tilt(w.r.t z)	1 degree	0.04
detector efficiency	0.0 - 1.0	0.1
detector noise	up to 20% of rate	0.1
fringe field	100%	0.05
radiative corrections	20%	0.05
DAQ inefficiency correction	40%	0.3
DAQ inefficiency pt.-to-pt.		0.3
Beam vert. pos. variation	0.5 mrad	0.2
helicity correl. beam pos.	5 nm	< 0.05
helicity correl. beam angle	3 mrad	< 0.05
spin precession in chicane	20 mrad	< 0.03
Total		0.59

The extensive simulation studies provided a compre-
 hensive list of contributions to the systematic uncer-
 tainties, as tabulated in Table I, with a net systemat-
 ic uncertainty of 0.59% for the Compton polarimeter. The
 extracted beam polarization for the entire second run-
 ning period is shown in Fig. 7. The results from the
 Compton polarimeter were also compared to the inter-
 mittent measurements made with the Møller polarimeter
 [2, 3] and two polarimeters were found to be consist-
 ent with each other within the systematic uncertainties
 of the measurements.

CONCLUSIONS

We have measured the electron beam polarization of
 a 1.16 GeV beam using a set of diamond micro-strip
 detectors for the first time. The high resolution of the
 detectors and their proximity to the primary beam helped

303 record a large fraction of the Compton electron spectrum,³²⁹
 304 spanning both sides of the zero crossing of the Compton³³⁰
 305 asymmetry for the first time. These detectors, coupled³³¹
 306 with a robust analysis technique and rigorous simulations³³²
 307 of the polarimeter and the DAQ system, produced a very³³³
 308 reliable, high precision measurement of the polarization³³⁴
 309 in a very high radiation environment. They demonstrate³³⁵
 310 that diamond micro-strip detectors are indeed a viable³³⁷
 311 option as tracking detectors, and they are the appropri-³³⁸
 312 ate choice for tracking detectors that are exposed to very³³⁹
 313 high radiation dosage. We have also demonstrated that it³⁴⁰
 314 is possible to achieve high precision with a Compton po-³⁴¹
 315 larimeter operated at beam energies as low as ~ 1 GeV.³⁴²
 316 This has very positive implications for the future PVES³⁴⁴
 317 program at the upgraded JLab.

318 ACKNOWLEDGMENTS

319 This work was funded in part by the U.S. Department³⁵⁰
 320 of Energy contract # AC05-06OR23177, under which³⁵¹
 321 Jefferson Science Associates, LLC operates Thomas Jef-³⁵²
 322 ferson National Accelerator Facility, and contract # DE-³⁵³
 323 FG02-07ER41528, and by the Natural Sciences and Engi-³⁵⁴
 324 neering Research Council of Canada (NSERC). We thank³⁵⁵
 325 H. Kagan from Ohio State University for teaching us³⁵⁶
 326 about diamonds, training us on characterizing them and³⁵⁷
 327 helping us build the proto-type detector.³⁵⁸

- [2] T. Allison *et al.*, Nucl. Instr. Meth. **A781**,105 (2015).
 [3] J. Magee, Proc. of Sci. PSTP2013, 039 (2013).
 [4] D. Gustavson *et al.* Nucl. Instr. Meth. **A165**, 177 (1979);
 L. Knudsen *et al.*, Phys. Lett. **B270**, 97 (1991).
 [5] D. P. Barber *et al.*, Nucl. Instr. Meth. **A329**, 79 (1993).
 [6] M. Woods, Proc. of the Workshop on High Energy Polarimeters,
 Amsterdam, eds. C. W. de Jager *et al.*, p. 843 (1996);
 SLAC-PUB-7319 (1996).
 [7] I. Passchier *et al.*, Nucl. Instr. Meth. **A414**, 446 (1998).
 [8] W. Franklin *et al.*, AIP Conf.Proc. 675, 1058 (2003).
 [9] M. Baylac *et al.*, Phys. Lett. **B539**, 8 (2002); N. Felletto
et al., Nucl. Instr. Meth. **A459**, 412 (2001).
 [10] A. Acha *et al.* [HAPPEX Collaboration], Phys. Rev. Lett.
98, 032301 (2007).
 [11] D. R. Kania, M. I. Landstrass and M. A. Plano, Diam.
 Relat. Mater. **2**, 1012 (1993).
 [12] R. Berman (ed), *Physical Properties of Diamond*, Oxford
 University Press, Oxford, 1965.
 [13] J. E. Field (ed), *The Properties of Diamond*, Academic,
 New York, 1979.
 [14] R. J. Tapper, Rep. Prog. Phys. **63**, 1273 (2000).
 [15] C. Bauer *et al.* Nucl. Instrum. Methods **367**, 207 (1995).
 [16] M. M. Zoeller *et al.*, IEEE Trans. Nucl. Sci. **44** 815
 (1997).
 [17] The CERN grade diamond plates were procured from
 Element Six, 35 West 45th St., New York, NY 10036,
 USA.
 [18] C.K. Sinclair *et al.*, Phys. Rev. ST Accel. Beams **10**,
 023501 (2007); P.A. Adderley *et al.*, Phys. Rev. ST Accel.
 Beams **13**, 010101 (2010).
 [19] CERN Program Library Long Write-up W5013, Unpub-
 lished (1993)
 [20] Modelsim Reference Manual, Mentor Graphics
 Corp.,Unpublished (2010).
 [21] V1495 modules from CAEN Technologies, Inc. 1140 Bay
 Street, Suite 2C, Staten Island, NY 10305 - USA

328 [1] D. Androic *et al.*, Phys. Rev. Lett. **111**, 121804 (2013).